CHAPTER 4

Colloidal ZnO QDs and CdSe QDs Based Inorganic Self-Powered Photodetectors*

Contents

*Part of this work has been published as:

Hemant Kumar et al. Electrical and Optical Characteristics of Self- Powered Colloidal CdSe Quantum Dot-Based Photodiode. *IEEE Journal of Quantum Electronics*, 53(3):1-8, 2017.

CHAPTER 4

Colloidal ZnO QDs and CdSe QDs Based Inorganic Self-Powered Photodetectors

4.1 Introduction

We have already discussed in chapter-1 self-powered photodetectors operate under photovoltaic mode without requiring any external power supply (Jin *et al.*, 2012; Gao *et al.*, 2013; Bera *et al.*, 2016)). The detailed literature review regarding the self-powered PDs has also been discussed in chapter-1. Although the inorganic semiconductors based self-powered PDs are lucrative due to their high mobility and high absorption coefficient (Bera *et al.*, 2016), the high-temperature fabrication process requirement is considered to be the major drawback of devices (Jin *et al.*, 2012; Gao *et al.*, 2013). Gao et al. (Gao *et al.*, 2013) and Jin et al. (Jin *et al.*, 2012) used CdSe nanobelts (NBs) to fabricate self-powered PDs at nearly 1000^{o}C to achieve a very high responsivity (>8 A/W). High-temperature processing consumes a lot of power and defeats the purpose of self-powered PDs. In this chapter, we have proposed a low-temperature processed colloidal ZnO and CdSe QDs based n-Si/ZnO QD/CdSe QD/Au self-powered PD structure. The device fabricated is on n-Si substrate as the device under study is analysed for the top side illumination and the ZnO QD thin film annealed at 250^{o}C (as optimized in chapter-2) is used as the ETL, and CdSe QD thin film is used as the active layer. Since optical properties of the colloidal ZnO QDs have already discussed in chapter-2, we have investigated the same for CdSe QDs in the present chapter. Au is used as a top electrode in self-powered PD which is equivalent to MoO_x/Ag (Brown *et al.*, 2011) and resolves the problem of solution processed and thermally grown MoO_x

discussed in chapter-3. Finally, the photoresponse and time-response characteristics of the Au/CdSe QDs Schottky PD grown on the ZnO QDs ETL have been analyzed for the visible spectrum under zero bias condition. The outline of this chapter is given as follows.

Section 4.2 discusses the complete fabrication details of the Au/CdSe QDs/ZnO QDs based self-powered PD under study. The result regarding optical and electrical properties of the materials and device are presented in Section 4.3. Finally, the conclusion and summary of the chapter are presented in Section 4.4.

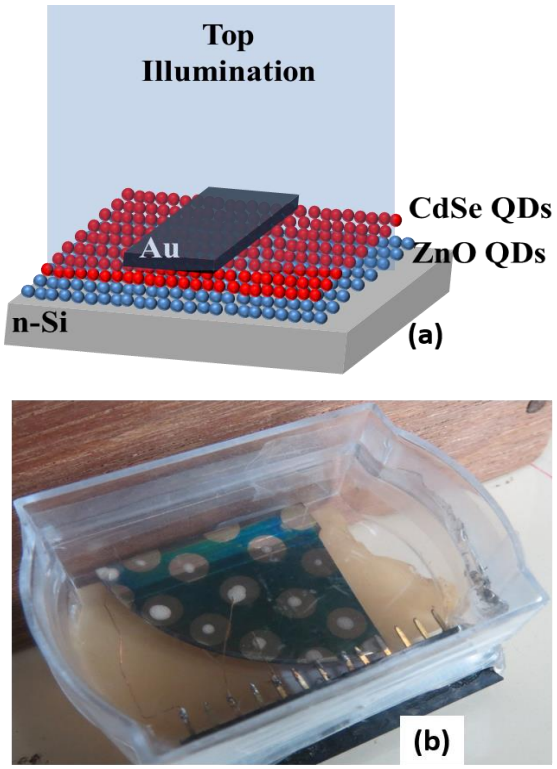

Figure 4.1: (a) Complete device schematic Au (~80 nm)/CdSe QDs (~30 nm)/ZnO QDs (~40 nm)/n−Si and (b) Fabricated and packaged device under consideration.

4.2 Experimental Details

The complete device structure schematic and fabricated device as considered in the present study is shown in Figure 4.1 (a) and (b). The CdSe and ZnO QDs thin film was

deposited on cleaned n-Si <111> substrate (the cleaning procedure is reported in (Rawat *et al.*, 2016)). The used chemicals were acquired from Merk India Ltd. and Sigma-Aldrich ≥ 99% purity. The fabrication of the device is described in following two steps.

4.2.1 Device Fabrication

QD Deposition: The prepared solution of ZnO QD is deposited on the cleaned n-Si substrate using spin coating (SPM-150LC, GmbH) at 3000 rpm and then dried at 150^{o}C. This process is repeated until the desired thickness of ~40 nm is achieved, which is measured using Reflectometer (F-20, Filmetrics). The ZnO QD deposited substrate is annealed in the ambient environment at 250^{o}C before the deposition of CdSe QDs as concluded in chapter 2. Afterwards, the prepared solution of CdSe QDs is spin-coated over the ZnO QDs deposited substrate at 1500 rpm, and then a coating of ethanedithiol (EDT) is performed as specified in chapter 2. This process is repeated until the thickness of CdSe QDs is achieved to be ~30 nm measured using Reflectometer.

Contact Deposition: High purity Au (99.9%) was deposited by thermal evaporation (HHV, FL400 SMART COAT 3.0 A) on the CdSe/ZnO QDs thin film. Vacuum deposition of Au (~80 nm) was performed at very high vacuum (~10^{-6} bar) at a very slow rate of 0.1 Å/s till 25 nm to obtain smooth and uniform film and remaining 55 nm deposited at the rate of 1.5 Å/s. The separation between the source and substrate was fixed for the complete deposition and maintained at ~18 cm. The circular Au contact is deposited with the help of shadow masking with the area of 0.12 cm^2. After the preparation of the device, silver paste is used for making contacts between probes and the devices. Where silver paste over Au is used as a top contact and silver paste over the scratched surface of n-Si is used as a back contact. Silver paste is also used to package the fabricated device as shown in Figure 4.1 (b).

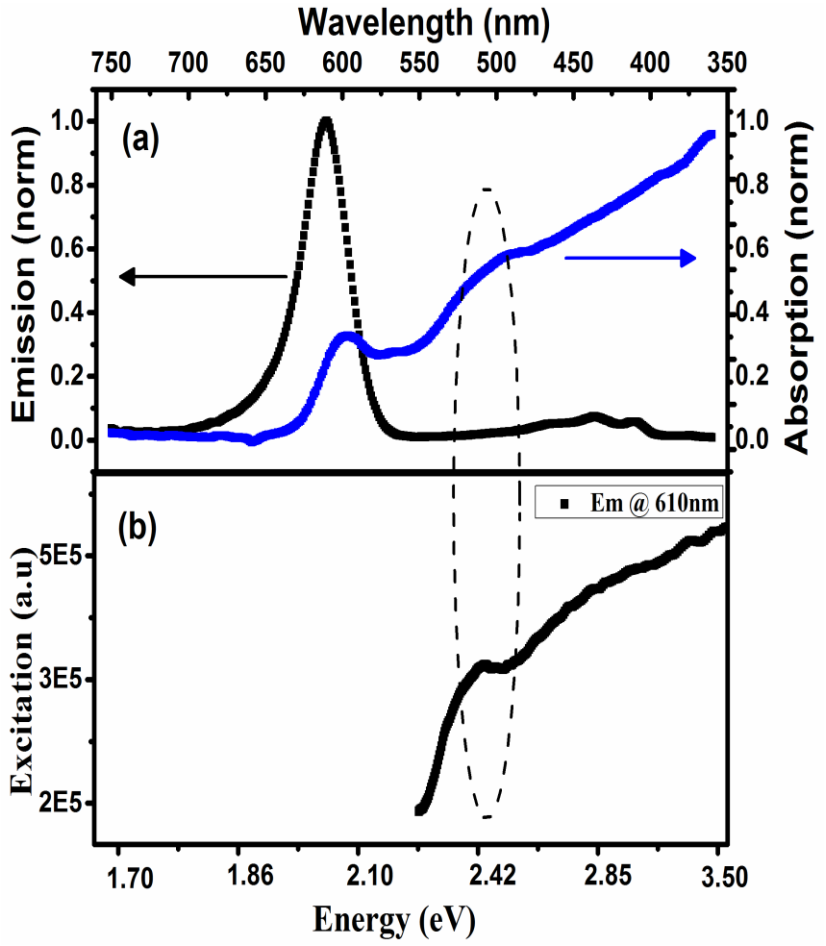

Figure 4.2: (a) Photoluminescence and absorption spectrum of colloidal CdSe QDs solution (b) Photoluminescence Excitation (PLE) spectrum of CdSe QDs for emission wavelength of 610nm (2.03eV).

4.3 Result and Discussion

In this section, the optical and electrical characteristics of the ZnO QD/CdSe QD based self-powered photodetector is discussed.

4.3.1 Optical Characterization

The study of the optical results of CdSe QDs and Au electrode is analyzed in this section. The Photoluminescence (PL) and absorption of CdSe QDs are shown in Figure 4.2 (a) using Edinburgh Photonics F980 and F-20, Filmetrics respectively. The sharp luminescence peak of CdSe QDs is observed at a 612 nm wavelength with a very

narrow full width at half maximum (FWHM) of 37.30 nm for the excitation wavelength of 335 nm. The selective and single peak of CdSe QDs exhibits the high quality of synthesized QDs. The PL of QDs are hugely affected by the surface and can be treated as surface effect as the surface to volume ratio of QDs are very high. Further, the quantized bandgap of QDs are also dependent upon the size of QDs as specified below (Klimov, 2010):

$$E_n = n^2\pi^2\hbar^2 / 2ma^2 \tag{4.1}$$

here *n*, *m*, *ħ*, and *a* is the quantum number, mass of the charge particle, Planck's constant divided by *2π*, and diameter of the QDs, respectively. These results are the interpretation of one direction only, which indicates the decrement in *a* leads to proportionate increase between the energy bands (E_n). For the case of QDs, an initial model of particle-in-a-box can be applied for the calculation of energy band states. Further, assuming the boundary condition and wave equation of particle in a box:

$$V(r) = \begin{cases} 0 \; r < a \\ \infty \; r > a \end{cases}, and \frac{d^2\Psi(r)}{dx^2} + \frac{2m}{\hbar^2} E\Psi(r) = 0 \tag{4.2}$$

solving the wave equation $\psi(r)$ or $\psi(x,y,z)$ for $E_n(x,y,z)$ we get:

$$E_n(x,y,z) = \frac{\pi^2\hbar^2}{2m}\left(\frac{n_x^2}{a_x^2} + \frac{n_y^2}{a_y^2} + \frac{n_z^2}{a_z^2}\right) \tag{4.3}$$

here the solution is only applicable to one particle (electron or hole). To analyze the model for multiple particles or to involve interaction among electron-hole pair, coulombic interaction (E_c) should be involved in Equation 4.3 the modified equation can be rewritten as:

$$E_n(x,y,z) = \frac{\pi^2\hbar^2}{2m}\left(\frac{n_x^2}{a_x^2} + \frac{n_y^2}{a_y^2} + \frac{n_z^2}{a_z^2}\right) - E_c \tag{4.4}$$

$$E_c = k_e q^2 \left(\frac{1}{b_x} + \frac{1}{b_y} + \frac{1}{b_z} \right) \quad (4.5)$$

where *b* is the natural separation of the electron-hole pair. Quantum size effect is evident if the size of the particle is less than the natural separation of electron-hole pair. Bohr's radius (~5.6 nm for CdSe QDs) can be approximated as the convenient scale for the same (Klimov, 2010). As the particle size (~4.84 nm) obtained for the CdSe QDs is less than the Bohr's radius and specify the prepared QDs are within the strong quantum confinement regime (Klimov, 2010). Further, assuming the values of a_x, a_y, and a_z are nearly equal as the particle size is nearly spherical:

$$a = a_x = a_y = a_z = 4.84/2 = 2.42 \text{ nm} \quad (4.6)$$

solving Equation 4.4 using the above details we get:

$$E_n(x, y, z) = a_0\left(n_x^2 + n_y^2 + n_z^2\right) - E_c \quad (4.7)$$

where a_o is constant of value 9.3×10^{-17}. Further, the energy bands can be split between conduction and valence band with the introduction of E_g (forbidden energy band gap). For CdSe QDs valance band is constituted by the *4p* orbital of Se which is six-fold degenerated while the conduction band is constituted by *5s* orbital of Cd which is only two-fold degenerated (Klimov, 2010) can be calculated from Equation 4.7. This six-fold degeneracy of valence band results into subband structure of the valence band (Klimov, 2010) ($p_{1/2}$ and $p_{3/2}$ where the subscript indicates angular momentum $J = l + s$ (Klimov, 2010)) clearly shown in both the absorption and PL Excitation (PLE) spectrum shown in Figure 4.2 (a) and (b). In Figure 4.2 (a) the first absorption peak of CdSe QDs achieved at ~600 nm is due to the transition between *1S(e)-1S$_{3/2}$(h)* and for the second absorption hump at ~510 nm is due to the transition between *1P(e)-1P$_{3/2}$(h)*. This degeneracy in the energy bands does not affect the quality of the PL as the emission is

only started from *1S(e)* irrespective of the absorption wavelength as shown in Figure 4.3.

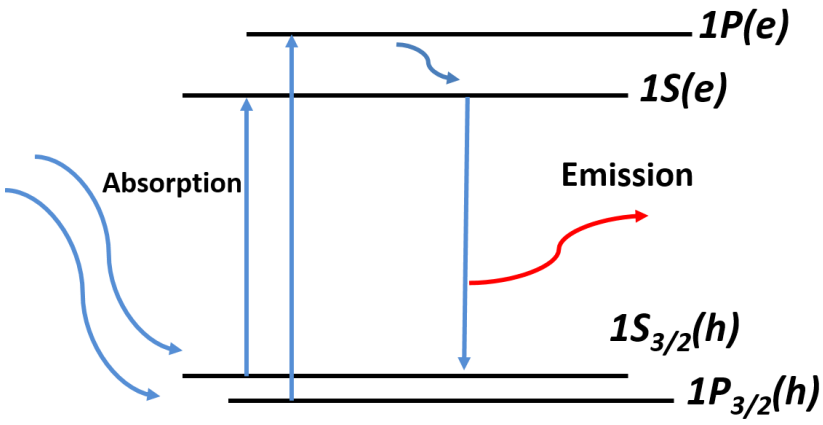

Figure 4.3: CdSe QD energy band levels with the depiction of absorption and photoluminescence between the energy states.

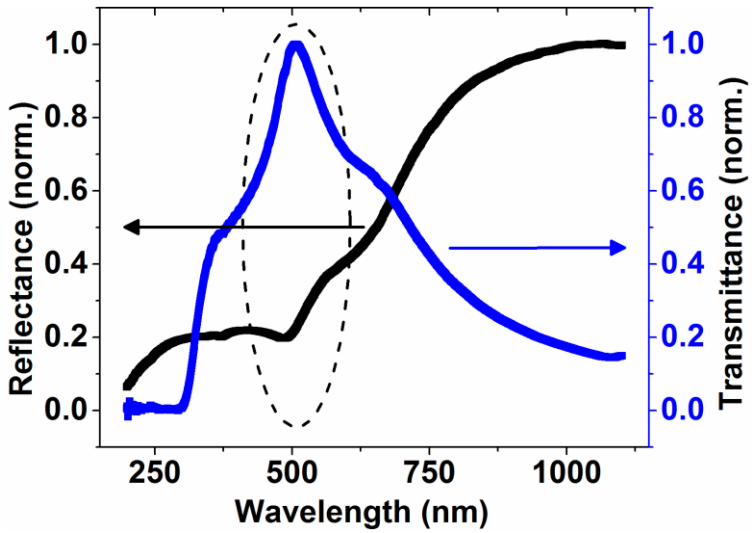

Figure 4.4: Reflectance and Transmittance normalized curve for gold thin film of thickness ~80 nm.

The CdSe Schottky photodiode prepared in this study is exposed from the top side, and it is mandatory to discuss the effect of Au electrode on the photoresponse of the photodiode. The reflectance and transmittance measured using Reflectometer (F-20, Filmetrics) of Au thin film as shown in Figure 4.4. The results clearly indicate that the Au thin film provides maximum transmittance and minimum reflectance over the

visible spectrum which is required for the operation of the Au/CdSe QDs based color photodiode.

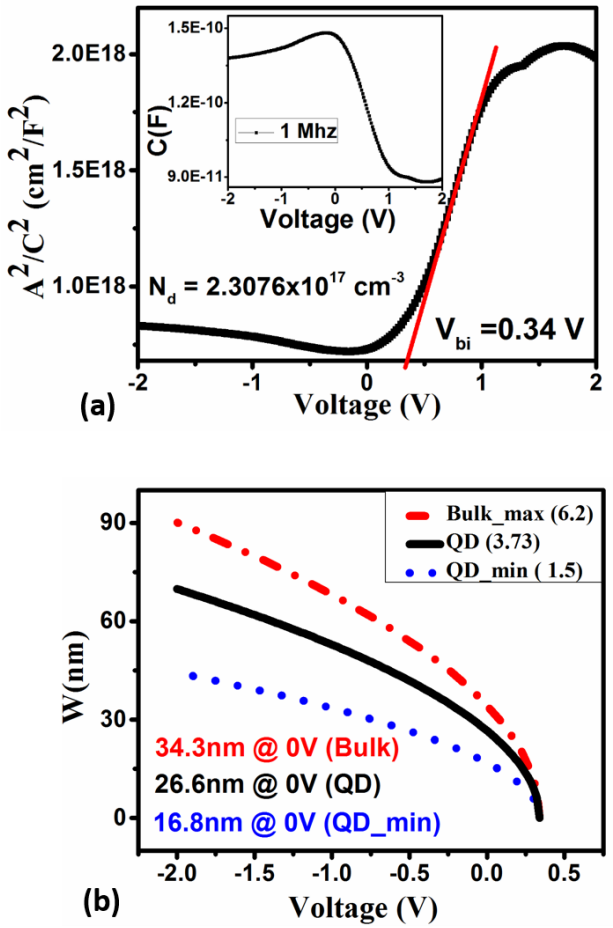

Figure 4.5: (a) A^2/C^2 vs. voltage characteristics for calculation of barrier height and carrier concentration with the inset of C-V curve, (b) Width of depletion region (W) vs. voltage for the different values of dielectric constant (bulk (Hui, 2000), prepared QDs, and small QDs (Hui, 2000)).

4.3.2 Electrical Characterization

C-V characterization: In this section, Au/CdSe QDs based Schottky diode is analyzed for the inverse capacitance versus voltage (A^2/C^2 vs. V) relationship shown in the Figure 4.5 (a), measured using Agilent B1500A from -2 V to +2 V. Further, the C-V plot is used to estimate the various parameters such as donor charge carrier density (N_d), width of depletion region (W), and built-in potential (ϕ) of Schottky photodiode. The Schottky junction is formed between Au and CdSe QDs and the complete depletion

region is extended into the CdSe QDs thin film. Now, we can use Equation 3.1 to analyze the data. From the projected intersection of capacitance curve in voltage axis, the value of built-in potential is found to be ~0.34 V. Further, the value of N_d calculated from the slope is 2.30×10^{17} cm^{-3}. Obtained data can be utilized for the calculation of W across the Schottky junction using the expression (Sze, 2002):

$$W = \sqrt{\frac{2\varepsilon_s(\phi - V)}{qN_d}} \tag{4.8}$$

The width of the depletion region is dependent upon the dielectric constant of the material and Ping (Hui, 2000) reported the variation in dielectric constant of CdSe QDs with the particle size. Ping (Hui, 2000) has reported dielectric constants for different size ranging from 0.5 - 3.5 nm and the dielectric constant reported for 0.5 nm is 1.5. Also, the maximum dielectric constant can be achieved for CdSe bulk is 6.2 (Hui, 2000). In the contrast of the above, we have calculated the dielectric constant of the prepared CdSe QDs using the refractive index (n) and extinction coefficient (k) calculated using Reflectometer (F-20, Filmetrics), values shown in Table 4.1.

Table 4.1: Measured values of n and k

Wavelength (nm)	n	k
435.8	1.9409	0.2048
632.8	1.9409	0.2048

The real part and imaginary part of the dielectric constant can be calculated using (Wooten, 1972):

$$\varepsilon_r = n^2 - k^2, \varepsilon_i = 2nk \tag{4.9}$$

The calculated values of ε_r = 3.73 and $\varepsilon_i = 0.79$ where the real part of dielectric constant specifies the energy stored within the medium and imaginary part specifies the loss due to attenuation within the medium. The dielectric constant is approximated to be 3.73 and the width of depletion region estimated using Equation 4.8 is shown in Figure 4.5 (b) for the different values of dielectric constants. The dielectric constant of bulk (6.2 (Hui, 2000)) provides the upper limit of the depletion region (W_{bulk} = ~34.3 nm at 0 bias). The dielectric constant of CdSe QDs with size 0.5 nm (1.5 (Hui, 2000)) provides the lower limit of the depletion region (W_{qd_min} = ~16.8 nm at 0 bias). The calculated value of dielectric constant of prepared CdSe QDs with a size of ~4.84 nm provides the width of the depletion region equals to ~26.6 nm at 0 bias. This result specifies that more than 85% of CdSe QDs (30 nm) thin film is depleted from the charge carriers, this depleted region which is under the junction electric field is responsible for the working of the self-powered Au/CdSe QDs based photodiode.

J-V characterization: The current density versus voltage (J-V) characteristics of Au/CdSe QDs Schottky photodiodes with ZnO QDs as an ETL is shown in the Fig. 7(a). The J-V characteristics of Au/CdSe QDs schottky diode without ZnO QDs as ETL is also shown in the inset of Figure 4.6 (a). The J-V characteristics of the devices are measured by using Agilent B1500A over bias voltage ranging from -1 V to +1 V. The photocurrent has been measured by using a white LED of fixed intensity of 96.8 μW/cm^2 at 500 nm. The Schottky photodiodes with ZnO QDs as an ETL clearly show the higher response and lower dark current as compared to those of devices without ZnO QDs interfacial layer or ETL. The lower dark current is achieved due to the increased thickness of the device by introduction of ZnO QDs as proposed by Ng et al. (Ng *et al.*, 2008). Further, the photoresponse of Schottky diode with ZnO QDs as an

ETL is 17 times higher than that of Au/CdSe QDs based device without using the ZnO QDs interlayer.

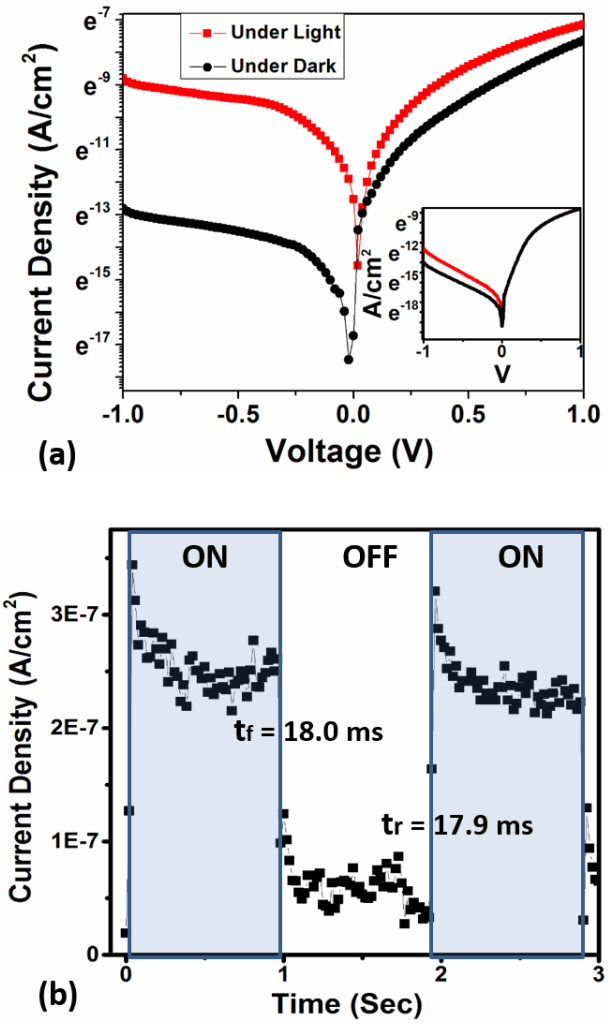

Figure 4.6: (a) J-V characteristics of the Pd/CdSe QDs Schottky diode with ZnO QDs as an ETL and without ZnO QDs layer in inset, (b) Time response characteristics of the Schottky diode for the light pulse of 1 sec without any applied bias.

The contrast ratio and the rectification ratio of the Schottky diode with ZnO QDs as ETL is calculated at an applied bias of -1 V found to be ~55 and 176 respectively. Further, The Schottky diode shows very low reverse saturation current density of 3.01×10^{-7} A/cm^2 with an ideality factor of 2.27 and effective barrier height of 0.67 eV using the Richardson constant of 15.6 Acm^{-2}K^{-2} (Tripathi, 2010). Electrical properties

of Schottky junction is compared with other reported works (Panchal *et al.*, 2007; Tripathi, 2010; Mahato, Shiwakoti and Kar, 2015) in Table 4.2.

Table 4.2: Comparison among the other reported CdSe Schottky diodes at room temperature.

Entities	**(Tripathi, 2010)**	**(Mahato, Shiwakoti and Kar, 2015)**	**(Panchal *et al.*, 2007)**	**This Work**	
Material Type	Bulk	Bulk	Bulk	CdSe QD	CdSe QD
Transport Layer	none	none	none	none	ZnO QD
Electrode	Au	Cu	Au	Au	Au
Barrier Height (ϕ_{bi}, eV)	0.485	0.46	0.63	0.66	0.67
Ideality factor (η)	3.9	4.8	4.7	2.48	2.27
Carrier Concentration (N_d ,cm^{-3})	-	-	2.1×10^{16}	3×10^{17}	2.30×10^{17}

Au/CdSe QDs with ZnO QDs as ETL based Schottky photodiode shows low reverse saturation current, superior ideality factor, and superior barrier height are due to the involvement of ~40 nm thick ZnO QDs thin film acting as an ETL and hole blocking layer as shown in Figure 4.7. The thickness of the active layer and involvement of ETL can reduce the leakage current and improve the device performance significantly as shown in Figure 4.6 (a). The electrical parameters of the Au/CdSe QDs Schottky diodes with and without the ETL layer have been compared with other reported works in Table 4.2. The electron affinity and ionization potential of ZnO QDs used is 4.34 eV and 7.76 eV, respectively. For the case of CdSe QDs electron affinity of 4.3 eV and the ionization potential of 6.5 eV is used (Oertel *et al.*, 2005). Further, the work function of Au electrode is assumed to be 5 eV (Pal *et al.*, 2012). The

response time characteristics of Schottky photodiode at an applied bias of zero volt is shown in the Figure 4.6 (b).

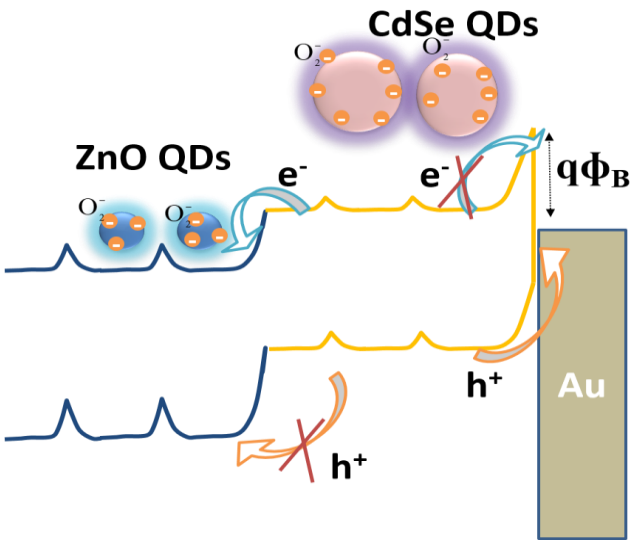

Figure 4.7: Charge distribution and energy band of Au/CdSe QD with ZnO QDs as an ETL.

The diode is excited with a square pulse of white light (96.8 μW/cm^2 at 500 nm) with a period of 1 sec. The Au/CdSe Schottky diode shows very fast response with a rise time ~17.9 ms and fall time of 18.0 ms without any applied bias. This fast response speed of Au/CdSe QDs based Schottky photodiode is attributed due to the introduction of barrier in-between the QDs as shown in Figure 4.7. Under the light exposure, there is a change in barrier height which increases the photocurrent. Further, the introduction of ZnO QDs with a particle size ~2.31 nm enhances the extraction of electrons from the depleted region while holes move via Au electrode under the influence of electric field present due to the built-in potential of junction also depicted in Figure 4.7. The larger photoresponse obtained in Figure 4.6 (a) can be attributed to the effect of efficient charge separation by the ETL as evidenced by Figure 4.7. Further, the figure of merit for the photodiodes responsivity (*Re*) and detectivity *(D*)* are also calculated at an applied bias of 0 V by using Equation 2.5 and Equation 2.6, respectively. The

photocurrent density of the self-powered Schottky photodiode is shown in Figure 4.8 (a) with an optical power density of the source. The responsivity and detectivity of the Au/CdSe QDs based photodiode are characterized from 300 nm to 750 nm as shown in Figure 4.8 (b).

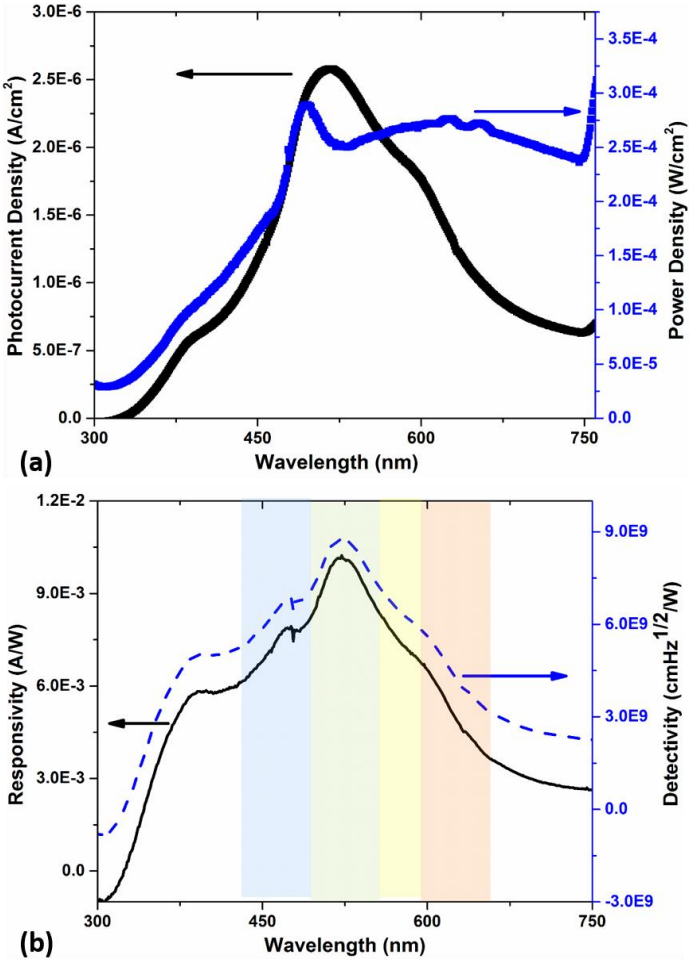

Figure 4.8: Photoresponse characteristics of self-powered Au/CdSe QDs based Schottky photodiode (a) Photocurrent density of device and optical power density plot of source against wavelength, (b) responsivity and detectivity of device against wavelength.

As explained earlier under the effect of built-in potential only the charge pairs generated in depletion region, i.e. CdSe QDs will participate in responsivity and detectivity. The photons absorbed by ZnO QDs will not participate in charge transport due to two reasons:

(i) ZnO QDs thin film is not under the effect of the electric field produced across the depletion region as the depletion region of Au/CdSe QDs based photodiode is extended towards the CdSe QDs and covers ~88% of the thin film. Hence, remaining 12% of CdSe QDs thin film and complete ZnO QDs thin film is not depleted. So the charge-pair generated in ZnO QDs will not separate and hence recombine again.

(ii) The Au/CdSe QDs based photodiode is illuminated from the top side, as the transmittance and reflectance of Au thin film shown in Figure 4.4 clearly indicate maximum transmission and minimum reflectance across ~500 nm. Further, Au thin film shows very low transmittance for short wavelengths which is acting as a filter for short wavelengths. This filter effect of Au thin film is also responsible for no photoresponse produced by ZnO QDs thin film.

The responsivity and detectivity at an applied bias of 0 V shown in Figure 4.8 (b) clearly shows the color sensitive nature of self-powered Au/CdSe QDs Schottky photodiode and the maximum responsivity of 10.23 mA/W and maximum detectivity of 8.81×10^9 $cmHz^{1/2}/W$ is achieved at a wavelength of 522 nm which falls in the green region of visible spectrum. A comparative study is provided in the Table 4.3 between other CdSe based self-powered photodetectors (Jin *et al.*, 2012; Gao *et al.*, 2013) and other reported CdSe QDs based photodetectors (Oertel *et al.*, 2005; Nusir *et al.*, 2014). The photoresponse parameters of CdSe QDs Schottky photodiodes without ZnO QDs based ETL have also been included in Table 4.3. The results clearly strengthen the claim that the ZnO QDs based ETL plays a significant role in extracting the charge carriers from the fully depleted CdSe QDs active layer to improve the responsivity and detectivity significantly as demonstrated in this paper. The self-powered photodetectors (Jin *et al.*, 2012; Gao *et al.*, 2013) shows very high responsivity but faces a major

drawback of high-temperature processing and also all the other compared work used very high illumination density for their detector response.

Table 4.3: Comparison among other reported CdSe QDs based photodetectors or CdSe based self-powered photodetectors.

Entities	**(Gao *et al.*, 2013)**	**(Jin *et al.*, 2012)**	**(Oertel *et al.*, 2005)**	**(Nusir *et al.*, 2014)**	**This Work**	
Material Used	CdSe NBs	CdSe NBs	CdSe QDs	CdSe NCs	CdSe QDs	CdSe QDs
Transport Layer	-	-	PEDOT: PSS	-	-	ZnO QDs
Self-powered	Yes	Yes	No	No	-	Yes
Operating Bias (V)	0	0	0	5	0	0
Responsivity (A/W)	8.7	10.2	-		5.47×10^{-4}	10.2×10^{-3}
Detectivity ($cmHz^{1/2}\cdot W^{-1}$)	-	-	-	3.5×10^{10}	4.72×10^{8}	8.81×10^{9}
Max. Temp used for device fabrication	1000ºC	1000ºC	110ºC	300ºC	80ºC	250ºC
Illumination Density	167 mW/cm^2	~2.7 mW/cm^2	110 mW/cm^2	350 mW/cm^2	0.25 mW/cm^2	
Deposition Techniques	Chemical Vapor Deposition (CVD)		Solution Processing			

Further, the table also states the low-cost implementation of CdSe QDs by solution processing compared to other techniques (CVD) used by (Jin *et al.*, 2012; Gao *et al.*, 2013) which requires sophisticated facilities.

4.4 Conclusion

In this work, a low-temperature processed self-powered Schottky photodiode of Au/CdSe QDs/ZnO QDs is studied for the first time over the visible spectrum with ZnO

QDs as the ETL and CdSe QDs as the active layer. The morphological and optical characteristics of the CdSe QDs have been investigated using TEM, PL, and absorption spectrum. The electrical parameters of Au/CdSe QDs based Schottky diode have been extracted from the measured I-V and C-V characteristics. The built-in potential, carrier density, and width of the depletion region at zero applied bias are obtained as 0.34 V, ~$2.30x10^{17}$ cm^{-3}, and ~26.9 nm, respectively while the ideality factor is found to be 2.27 with the effective barrier height of 0.67 eV. The photoresponse of the device is also discussed using the measurements like time-response, responsivity (10.23 mA/W), and detectivity (8.81×10^{9} $cmHz^{1/2}/W$). The rise time and fall time of the Schottky photodiode is found to be 17.9 ms and 18.0 ms, respectively. It is believed that the present work could be stepping stone towards the development of colloidal QDs based low-cost and large area self-power photodetectors.